

On Intersecting Conformal Defects

Tom Shachar

*The Racah Institute of Physics, The Hebrew University of Jerusalem,
Jerusalem 91904, Israel*

E-mail: tom.shachar@mail.huji.ac.il

ABSTRACT: We study the physics of 2 and 3 mutually intersecting conformal defects forming wedges and corners in general dimension. For 2 defects we derive the beta function of the edge interactions for infinite and semi-infinite wedges and study them in the tricritical model in $d = 3 - \epsilon$ as an example. We discuss the dependency of the edge anomalous dimension on the intersection angle, connecting to an old issue known in the literature. Additionally, we study trihedral corners formed by 3 planes and compute the corner anomalous dimension, which can be considered as a higher-dimensional analog of the cusp anomalous dimension. We also study 3-line corners related to the three-body potential of point-like impurities.

Contents

1	Introduction	1
2	Two Defects: RG on the Edge	4
2.1	Semi-Infinite Plane	4
2.2	Two Intersecting Planes	6
2.3	Wedge Formed by Two Semi-Infinite planes	8
2.4	Example: $(\phi^4)_{\mathcal{D}_1} \cap (\phi^4)_{\mathcal{D}_2} : (\phi^2)_{\mathcal{I}}$ in Tricritical Bulk	10
3	Three Defects: Trihedral & 3-Line Corners	15
3.1	Trihedral Corners	15
3.2	The 3-Line Potential	18
4	Discussion	21
A	List of Integrals	22

1 Introduction

Defects in QFT and lattice systems is a vast and rapidly growing field. A particularly well-studied kind are defects that are created by altering the interactions on some lower-dimensional surface inside the bulk. From the CFT perspective, they can be thought of as local deformations of conformal theories, confined to some sub-manifold. Many interesting universality classes can be explored in this way, usually by deforming a bulk CFT or BCFT/DCFT with conformal boundary conditions such as Dirichlet or Neumann. This approach enjoys access to powerful tools such as Bootstrap, epsilon expansion, and large N methods [1–43].

In this paper we inquire about what happens when defects meet. We will be able to answer this question and compute new quantities by using the OPE, combined with conformal perturbation theory. Qualitatively, divergences arise when operators from two or more different defects collide at their intersection. These divergences will drive an RG flow localized to the intersection and consequently augment the degrees of freedom in that region. Specifically, it is possible to generate perturbative flows if an operator with a scaling dimension close to the dimension of the intersection is present

in the OPE of the two defects. More so, the same effect happens on a single defect when operators collide on its boundary, which to avoid possible confusion we refer to as its edge. There is therefore an abundance of different geometric constructs that may be considered, since the intersection can serve as the edge of some or all of the defects in the picture. In this manuscript we shall explore among the rest the planar geometries depicted in Fig. 1. CFT on the wedge has been explored in the older literature [44–58], as well as in contemporary one under broader contexts [59–71]. We also mention works done on conformal interfaces and RG defects [72–85].

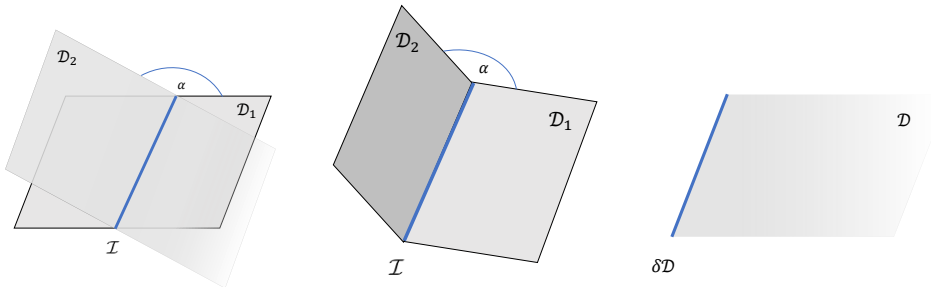


Figure 1. Examples of the defect geometries explored in section 2. The edge $\delta\mathcal{D}$ or the intersection \mathcal{I} are marked with a thick blue line, and α is the intersection angle. For the wedge (middle picture), the intersection is also the common edge of the two planes.

To exemplify this idea we study perturbative flows in the tricritical model in $d = 3 - \epsilon$ dimensions. For illustration, consider the action (see Fig. 1),

$$S = \int d^{3-\epsilon}x \left(\frac{1}{2} (\partial\phi)^2 + \lambda\phi^6 \right) + g^{(1)} \int_{\mathcal{D}_1} d^{2-\epsilon}x \phi^4 + g^{(2)} \int_{\mathcal{D}_2} d^{2-\epsilon}x \phi^4 + h \int_{\mathcal{I}} d^{1-\epsilon}x \phi^2. \quad (1.1)$$

We study this type of actions for the 3 geometries shown in Fig. 1 and for two different sets of defect dimensions for both interacting and non-interacting bulk. All of the results are tabulated and discussed in part 2.4. Among other things, we shall discuss the interesting dependence of the critical edge coupling h^* on the intersection angle α .

We may even proceed further and explore more complicated objects, such as three mutually intersecting defects. Fortunately, conformal perturbation analysis is still applicable when the mutual intersection of the three defects is a point. Namely, a corner, as portrayed in Fig. 2. At criticality, a central feature of this object is the anomaly in the scaling symmetry around the fixed corner point, which originates from the geometric singularity at the corner. One of the most important results is obtained for the trihedral corner, a corner formed by three intersecting 2-dimensional planes. The defects are defined by the deformations $\sum_{a=1}^3 g^{(a)} \int_{\mathcal{D}_a} d^2x \mathcal{O}_a$, and for weak couplings the

anomaly arises from a specific term in the cubic order through a logarithmic divergence in the free energy,

$$\log Z = -\Gamma_{\text{corner}} \log\left(\frac{L}{a}\right) \cdots = -g^{(1)}g^{(2)}g^{(3)} \int_{\mathcal{D}_1} \int_{\mathcal{D}_2} \int_{\mathcal{D}_3} \langle \mathcal{O}_1 \mathcal{O}_2 \mathcal{O}_3 \rangle + \dots \quad (1.2)$$

For the extended trihedral corner (see Fig. 2), the cubic order gives the leading contribution to the anomaly, which we deem as the corner anomalous dimension, Γ_{corner} . It can be considered therefore as a higher dimensional analog of the cusp anomalous dimension [67, 86, 87].

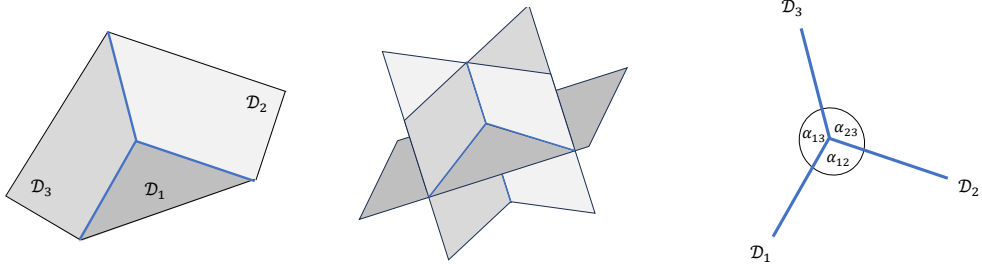


Figure 2. The objects studied in section 3. *Left:* Trihedral Corner. *Middle:* Extended Trihedral Corner. *Right:* 3-line Corner. The planes meet at a mutual point, giving rise to the corner anomaly depending upon the three relative angles of the edges, $\alpha_{12}, \alpha_{23}, \alpha_{13}$.

For the extended version of the trihedral corner discussed in part 3.1 we find,

$$\Gamma_{\text{corner}}(\alpha_{12}, \alpha_{23}, \alpha_{13}) = \frac{\sin(\alpha_{12}) \sin(\alpha_{23}) \sin(\alpha_{13})}{V^2(\alpha_{12}, \alpha_{23}, \alpha_{13})} 4\pi^4 C g^{(1)} g^{(2)} g^{(3)}, \quad (1.3)$$

Where C is the OPE coefficient of the three defect deformations and V is the volume of the unit Parallelepiped entrapped inside the edges of the trihedron,

$$V^2 = 1 + 2 \cos(\alpha_{12}) \cos(\alpha_{13}) \cos(\alpha_{23}) - \cos^2(\alpha_{12}) - \cos^2(\alpha_{13}) - \cos^2(\alpha_{23}). \quad (1.4)$$

Corners can also be formed by 3 line defects. In such case, the corner contribution (1.2) to the anomalous dimension will be sub-leading to the cusp anomalous dimension that arises beforehand at second order,

$$\Gamma = \sum_{a < b}^3 \Gamma_{\text{cusp}}(\alpha_{ab}) + \Gamma_{\text{3-line}}(\alpha_{12}, \alpha_{23}, \alpha_{13}). \quad (1.5)$$

We may view each line defect as the world-line of a point-like impurity via conformal mapping to the cylinder $\mathbb{R} \times S^{d-1}$ [45, 67]. In this interpretation, we can think of $\Gamma_{\text{3-line}}$

as the three-body potential of impurities living on S^{d-1} . In part 3.2 we find an analytic closed-form expression for this object involving elliptic integrals, and study some of its properties.

The rest of the paper is organized as follows: In section 2 we use OPE to derive the running couplings and beta functions for a semi-infinite planar defect 2.1, two intersecting planes 2.2 and a wedge composed of two semi-infinite planes 2.3. In part 2.4 we finish with an example of the tricritical model in $d = 3 - \epsilon$ with ϕ^4 and ϕ^2 interactions localized to the planes and the edge respectively. In section 3 we introduce and briefly discuss the corner anomaly. In part 3.1 we define the trihedral corner and compute the corner anomalous dimension for its extended version. Subsequently, in part 3.2 the 3-line potential is defined and fully computed. Finally, we conclude the paper with a discussion.

2 Two Defects: RG on the Edge

In this section, we use scalar (zero-spin) primary operators of the bulk CFT algebra to construct three different geometric setups involving planar defects (see Fig. 1). We then use the OPE technique [88–91] to derive the beta functions of the edge and intersection couplings for all three setups.

In addition to the interaction terms studied here, non-flat intersections will have additional curvature terms generated in the RG flow, and their derivation is left outside the scope of this paper. It is also important to note that operators with non-zero spin may appear in the OPE of two scalars, and while their contributions to the running couplings vanish in the bulk due to rotational invariance, this is not necessarily the case here. While these new terms are interesting, they will be absent in the example we shall consider, and they are left outside the scope of our analysis for this time.

2.1 Semi-Infinite Plane

Consider a p -dimensional semi-infinite planar defect \mathcal{D} embedded in \mathbb{R}^d . Coordinates are chosen such that the defect is parameterized by the first p coordinates, with its edge at $x_p = 0$,

$$\mathcal{D} : (x_1, \dots, x_p, 0, 0, \dots, 0), \quad x_p \geq 0. \quad (2.1)$$

We write the following bare action,

$$S = S_{\text{CFT}} + g_{i,0} \int_{\mathcal{D}} d^p x \mathcal{O}_i(\vec{x}_{p-1}, x_p) + h_{\alpha,0} \int_{\partial\mathcal{D}} d^{p-1} x \mathcal{O}_\alpha(\vec{x}_{p-1}, 0), \quad (2.2)$$

Where for brevity we denoted $\vec{x}_{p-1} = (x_1, \dots, x_{p-1})$. For future convenience, we use Latin indices to list the set of scalar operators deforming the defect, and Greek indices for the ones on its edge, $\delta\mathcal{D}$.

In order to determine the RG flow perturbatively, we expand (2.2),

$$e^{-S} = e^{-S_{CFT}} \left(1 - g_{i,0} \int_{\mathcal{D}} d^p x \mathcal{O}_i - h_{\alpha,0} \int_{\partial\mathcal{D}} d^{p-1} x \mathcal{O}_\alpha + \frac{1}{2} g_{i,0} g_{j,0} \int_{\mathcal{D}} \int_{\mathcal{D}} \mathcal{O}_i \mathcal{O}_j + \frac{1}{2} h_{\alpha,0} h_{\beta,0} \int_{\partial\mathcal{D}} \int_{\partial\mathcal{D}} \mathcal{O}_\alpha \mathcal{O}_\beta + h_{\alpha,0} g_{i,0} \int_{\mathcal{D}} \int_{\partial\mathcal{D}} \mathcal{O}_i \mathcal{O}_\alpha + \dots \right). \quad (2.3)$$

A novelty of this construction is a divergent boundary contribution that appears in the $g^2 \int_{\mathcal{D}} \int_{\mathcal{D}} \mathcal{O}_i \mathcal{O}_j$ term which contributes to the renormalization of the edge couplings h_α . To see this, we perform an OPE of $\mathcal{O}_i(x) \mathcal{O}_j(y)$ around the point x and regularize the integral over y by removing a small cylindrical "pillbox" of size μ^{-1} around point x ,

$$\begin{aligned} \int_{\mathcal{D}} \int_{\mathcal{D}} \mathcal{O}_i(x) \mathcal{O}_j(y) &= \\ &= \int d^{p-1} x \int_{|\vec{y}_{p-1} - \vec{x}_{p-1}| \geq \mu^{-1}} d^{p-1} y \int_{x_p > 0} dx_p \int_{y_p > 0}^{y_p - x_p \geq \mu^{-1}} dy_p \frac{C_{ij}^k \mathcal{O}_k(\vec{x}_{p-1}, x_p)}{|x - y|^{\Delta_{ijk}}} + \dots \end{aligned} \quad (2.4)$$

Where C_{ij}^k are the OPE coefficients of the bulk CFT and $\Delta_{ijk} = \Delta_i + \Delta_j - \Delta_k$.¹ For slightly relevant operators with dimensions $\Delta_i, \Delta_j, \Delta_k$ all close to p , this leads to the usual logarithmic divergence that sets the running of the defect couplings g_i . Additionally, when $x_p < \mu^{-1}$, the removed pillbox is truncated at the edge at $y_p = 0$ and gives an additional boundary contribution. It is obtained from (2.4) by first integrating over \vec{y}_{p-1} with formula (A.1), and then taking the lower bound on $y_p = 0$ of the remaining integral over y_p that gives,

$$\begin{aligned} \int_{\mathcal{D}} \int_{\mathcal{D}} \mathcal{O}_i(x) \mathcal{O}_j(y) &= \\ &= \left(-\frac{\pi^{\frac{p-1}{2}} \Gamma\left(\frac{\Delta_{ijk} - p + 1}{2}\right)}{(\Delta_{ijk} - p) \Gamma\left(\frac{\Delta_{ijk}}{2}\right)} \right) \times \int d^{p-1} x \int_0^\infty dx_p \frac{C_{ij}^k \mathcal{O}_k(\vec{x}_{p-1}, x_p)}{|x_p|^{\Delta_{ijk} - p}} + \dots \end{aligned} \quad (2.5)$$

It is evident from (2.5) that divergences can appear as the operator approaches the edge $x_p \rightarrow 0$. We perform a partial Taylor expansion of the operator \mathcal{O}_k around $x_p = 0$

¹Indices will be freely raised and lowered with δ_{ij} without changing the value of the OPE coefficients.

and keep the zero order term,²

$$\begin{aligned} \int_{\mathcal{D}} \int_{\mathcal{D}} \mathcal{O}_i(x) \mathcal{O}_j(y) &= \\ &= \left(-\frac{\pi^{\frac{p-1}{2}} \Gamma\left(\frac{\Delta_{ij\alpha}-p+1}{2}\right)}{(\Delta_{ijk}-p) \Gamma\left(\frac{\Delta_{ij\alpha}}{2}\right)} \int_{\mu^{-1}}^{\infty} dx_p \frac{1}{|x_p|^{\Delta_{ij\alpha}-p}} \right) \times \int d^{p-1}x C_{ij}^{\alpha} \mathcal{O}_{\alpha}(\vec{x}_{p-1}, 0) + \dots \end{aligned} \quad (2.6)$$

Notice that now that the operator in (2.6) is set on the edge we have switched the index k to α . We see that divergences will arise when operators with dimension $\Delta_{\alpha} < p + 1 - \Delta_i - \Delta_j$ are present in the OPE of $\mathcal{O}_i \mathcal{O}_j$. We focus on perturbative flows, assuming slightly relevant deformations with dimensions $\Delta_i = p - \epsilon_i$ and $\Delta_{\alpha} = p - 1 - \epsilon_{\alpha}$. Other than (2.6), the divergences contributing to the renormalization of h_{α} come from the other terms in (2.3) and are not unusual (see *e.g.* [8]).³ In conclusion, we define the following renormalized coupling constant,

$$\begin{aligned} h_{\alpha} \mu^{\epsilon_{\alpha}} &= h_{\alpha,0} - \frac{\pi^{\frac{p-1}{2}} C_{\alpha}^{\beta\gamma} \mu^{-\epsilon_{\alpha}}}{\Gamma\left(\frac{p-1}{2}\right) \epsilon_{\alpha}} h_{\beta,0} h_{\gamma,0} - \frac{C_{\alpha}^{i\beta} \mu^{-\epsilon_i}}{\epsilon_i} \frac{\pi^{\frac{p}{2}}}{\Gamma\left(\frac{p}{2}\right)} g_{i,0} h_{\beta,0} + \frac{\pi^{\frac{p-1}{2}} C_{\alpha}^{ij} \mu^{-\epsilon_{ij\alpha}}}{2\Gamma\left(\frac{p+1}{2}\right) \epsilon_{ij\alpha}} g_{i,0} g_{j,0} \\ &+ \mathcal{O}(h^3, gh^2, g^2h, g^3), \end{aligned} \quad (2.7)$$

Leading to the following beta function for the edge couplings,

$$\beta_{\alpha} = -\epsilon_{\alpha} h_{\alpha} + \frac{\pi^{\frac{p-1}{2}} C_{\alpha}^{\beta\gamma}}{\Gamma\left(\frac{p-1}{2}\right)} h_{\beta} h_{\gamma} + \frac{\pi^{\frac{p}{2}} C_{\alpha}^{i\beta}}{\Gamma\left(\frac{p}{2}\right)} g_i h_{\beta} - \frac{\pi^{\frac{p-1}{2}} C_{\alpha}^{ij}}{2\Gamma\left(\frac{p+1}{2}\right)} g_i g_j. \quad (2.8)$$

Finally, the beta functions for the couplings g_i are standard and independent of (2.8),

$$\beta_i = -\epsilon_i g_i + \frac{\pi^{\frac{p}{2}} C_i^{jk}}{\Gamma\left(\frac{p}{2}\right)} g_j g_k. \quad (2.9)$$

2.2 Two Intersecting Planes

Consider two intersecting planar defects $\mathcal{D}_1, \mathcal{D}_2$ embedded in \mathbb{R}^d . We denote their intersection by $\mathcal{I} = \mathcal{D}_1 \cap \mathcal{D}_2$, having dimension $\dim(\mathcal{I}) = p - 1$. We choose a set of Cartesian coordinates such that \mathcal{I} lies in the first $p - 1$ coordinates, and in the (x_p, x_{p+1}) space the two planes are tilted by a relative angle α with respect to each other. For greater generality, we also allow one of the planes, arbitrarily chosen to be \mathcal{D}_2 , to extend

²An alternative derivation can be done by performing the OPE around the point $x = (\vec{x}_{p-1}, 0)$.

³There is a factor of half in the $\int_{\mathcal{D}} \int_{\partial\mathcal{D}} \mathcal{O}_i \mathcal{O}_{\alpha}$ contribution to (2.7) because the planar defect \mathcal{D} is semi-infinite.

in r additional transverse directions. Overall, $\dim(\mathcal{D}_1) = p$, $\dim(\mathcal{D}_2) = p + r$, and the defects are parameterized as follows,

$$\begin{aligned}\mathcal{D}_1 &: (x_1, \dots, x_{p-1}, x_p, 0, 0, \dots, 0). \\ \mathcal{D}_2 &: (y_1, \dots, y_{p-1}, y_p \cos \alpha, y_p \sin \alpha, y_{p+1}, \dots, y_{p+r}, 0, 0, \dots, 0).\end{aligned}\quad (2.10)$$

Given such choice, the distance between two points $x \in \mathcal{D}_1$, $y \in \mathcal{D}_2$ is given by,

$$|x - y|^2 = \vec{y}_r^2 + (\vec{x}_{p-1} - \vec{y}_{p-1})^2 + (x_p - y_p \cos \alpha)^2 + y_p^2 \sin^2 \alpha. \quad (2.11)$$

Where for brevity we denoted $\vec{y}_{p-1} = (y_1, \dots, y_{p-1})$ and $\vec{y}_r = (y_{p+1}, \dots, y_{p+r})$. As we anticipate that interactions localized on \mathcal{I} will be generated in the RG flow, we write the following general bare action,

$$S = S_{\text{CFT}} + g_{i,0}^{(1)} \int_{\mathcal{D}_1} d^p x \mathcal{O}_i(x) + g_{i,0}^{(2)} \int_{\mathcal{D}_2} d^{p+r} y \mathcal{O}_i(y) + h_{\alpha,0} \int_{\mathcal{I}} d^{p-1} x \mathcal{O}_\alpha(\vec{x}_{p-1}, 0), \quad (2.12)$$

Where for future convenience, we use Latin indices to list the scalar operators deforming the two defects and Greek indices for ones on the intersection. To determine the RG flow, we now expand,

$$e^{-S} = e^{-S_{\text{CFT}}} (1 - \delta S_1 - \delta S_2 - \delta S_{\mathcal{I}}), \quad (2.13)$$

Where

$$\delta S_1 = g_{i,0}^{(1)} \int_{\mathcal{D}_1} d^p x \mathcal{O}_i - \frac{1}{2} g_{i,0}^{(1)} g_{j,0}^{(1)} \int_{\mathcal{D}_1} \int_{\mathcal{D}_1} \mathcal{O}_i \mathcal{O}_j + \dots \quad (2.14)$$

$$\delta S_2 = g_{i,0}^{(2)} \int_{\mathcal{D}_2} d^{p+r} y \mathcal{O}_i - \frac{1}{2} g_{i,0}^{(2)} g_{j,0}^{(2)} \int_{\mathcal{D}_2} \int_{\mathcal{D}_2} \mathcal{O}_i \mathcal{O}_j + \dots$$

$$\begin{aligned}\delta S_{\mathcal{I}} &= h_{\alpha,0} \int_{\mathcal{I}} d^{p-1} x \mathcal{O}_\alpha - \frac{1}{2} h_{\alpha,0} h_{\beta,0} \int_{\mathcal{I}} \int_{\mathcal{I}} \mathcal{O}_\alpha \mathcal{O}_\beta \\ &\quad - h_{\alpha,0} g_{i,0}^{(1)} \int_{\mathcal{D}_1} \int_{\mathcal{I}} \mathcal{O}_\alpha \mathcal{O}_i - h_{\alpha,0} g_{i,0}^{(2)} \int_{\mathcal{D}_2} \int_{\mathcal{I}} \mathcal{O}_\alpha \mathcal{O}_i - g_{i,0}^{(1)} g_{j,0}^{(2)} \int_{\mathcal{D}_1} \int_{\mathcal{D}_2} \mathcal{O}_i \mathcal{O}_j + \dots\end{aligned}\quad (2.15)$$

Most of the divergences are standard, with an exception of a novel divergence that arises in the term $\int_{\mathcal{D}_1} \int_{\mathcal{D}_2} \mathcal{O}_i \mathcal{O}_j$ that occurs when the two operators collide at the intersection. We explore this in more detail by performing an OPE of $\mathcal{O}_i(x) \mathcal{O}_j(y)$ around the point $x = (\vec{x}_{p-1}, 0)$,

$$\int_{\mathcal{D}_1} \int_{\mathcal{D}_2} \mathcal{O}_i \mathcal{O}_j = \int d^{p-1} x \int d^{p-1} y \int dx_p \int dy_p \int d^r y \frac{C_{ij}^\alpha \mathcal{O}_\alpha(\vec{x}_{p-1}, 0)}{|x - y|^{\Delta_{ij\alpha}}} + \dots \quad (2.16)$$

By writing $|x - y|$ explicitly with (2.11) and using (A.1), we first integrate over $\vec{y}_r, \vec{x}_{p-1}, x_p$, and then introduce a UV cutoff to the resulting integral.⁴ We get,

$$\int_{\mathcal{D}_1} \int_{\mathcal{D}_2} \mathcal{O}_i \mathcal{O}_j = \left(\frac{2\pi^{\frac{p+r}{2}} \Gamma\left(\frac{\Delta_{ij\alpha} - p - r}{2}\right)}{\sin \alpha \Gamma\left(\frac{\Delta_{ij\alpha}}{2}\right)} \int_{\mu^{-1}}^{\infty} dy \frac{1}{y^{\Delta_{ij\alpha} - p - r}} \right) \times \int d^{p-1}x C_{ij}^{\alpha} \mathcal{O}_{\alpha}(\vec{x}_{p-1}, 0) + \dots \quad (2.17)$$

We focus on perturbative flows, assuming slightly relevant operators deforming \mathcal{D}_1 with dimensions $\Delta_i = p - \epsilon_i$ and likewise for \mathcal{D}_2 with dimensions $\Delta_j = p + r - \epsilon_j$. Divergent contribution appears in (2.17) for operators satisfying $\Delta_{\alpha} < \Delta_i + \Delta_j - p - r - 1$, and as consequence weakly relevant deformations on \mathcal{I} will be turned on for operators with $\Delta_{\alpha} = p - 1 - \epsilon_{\alpha}$, if they appear in the OPE of $\mathcal{O}_i \mathcal{O}_j$. Thus we define the renormalized couplings,

$$\begin{aligned} h_{\alpha} \mu^{\epsilon_{\alpha}} = & h_{\alpha,0} - \frac{\pi^{\frac{p-1}{2}} C_{\alpha}^{\beta\gamma} \mu^{-\epsilon_{\alpha}}}{\Gamma\left(\frac{p-1}{2}\right) \epsilon_{\alpha}} h_{\beta,0} h_{\gamma,0} - \frac{C_{\alpha}^{\beta i} \mu^{-\epsilon_i}}{\epsilon_i} h_{\beta,0} \left(\frac{2\pi^{\frac{p}{2}}}{\Gamma\left(\frac{p}{2}\right)} g_{i,0}^{(1)} + \frac{2\pi^{\frac{p+r}{2}}}{\Gamma\left(\frac{p+r}{2}\right)} g_{i,0}^{(2)} \right) \\ & - \frac{1}{\Gamma\left(\frac{p+r+1}{2}\right)} \frac{2\pi^{\frac{p+r+1}{2}} C_{\alpha}^{ij} \mu^{-\epsilon_{ij\alpha}}}{\sin \alpha \epsilon_{ij\alpha}} g_{i,0}^{(1)} g_{j,0}^{(2)} + \dots \end{aligned} \quad (2.18)$$

That lead to the following beta function,

$$\begin{aligned} \beta_{\alpha} = & -\epsilon_{\alpha} h_{\alpha} + \frac{\pi^{\frac{p-1}{2}} C_{\alpha}^{\beta\gamma}}{\Gamma\left(\frac{p-1}{2}\right)} h_{\beta} h_{\gamma} + C_{\alpha}^{\beta i} h_{\beta} \left(\frac{2\pi^{\frac{p}{2}}}{\Gamma\left(\frac{p}{2}\right)} g_i^{(1)} + \frac{2\pi^{\frac{p+r}{2}}}{\Gamma\left(\frac{p+r}{2}\right)} g_i^{(2)} \right) + \\ & + \frac{C_{\alpha}^{ij}}{\Gamma\left(\frac{p+r+1}{2}\right)} \frac{2\pi^{\frac{p+r+1}{2}}}{\sin \alpha} g_i^{(1)} g_j^{(2)}. \end{aligned} \quad (2.19)$$

Finally, independently of (2.19) the beta functions for the defect coupling constants $g^{(1)}, g^{(2)}$ assume the standard form,

$$\beta_i^{(1)} = -\epsilon_i g_i^{(1)} + \frac{\pi^{\frac{p}{2}} C_i^{jk}}{\Gamma\left(\frac{p}{2}\right)} g_j^{(1)} g_k^{(1)}, \quad \beta_i^{(2)} = -\epsilon_i g_i^{(2)} + \frac{\pi^{\frac{p+r}{2}} C_i^{jk}}{\Gamma\left(\frac{p+r}{2}\right)} g_j^{(2)} g_k^{(2)}. \quad (2.20)$$

2.3 Wedge Formed by Two Semi-Infinite planes

Consider a wedge that is formed by two semi-infinite p -dimensional planar defects that intersect at a mutual edge \mathcal{I} . This object is in principle a combination of parts 2.1 and

⁴In principle, we could regulate the integrals over $\vec{y}_r, \vec{x}_{p-1}, x_p$ as well, but in the scheme that we use we simply integrate these coordinate away. The universal logarithmic divergences are not sensitive to the choice of regularization scheme.

2.2. We use the former parameterization (2.10) to describe the defects,

$$\begin{aligned}\mathcal{D}_1 &: (x_1, \dots, x_{p-1}, x_p, 0, 0, \dots, 0), & x_p \geq 0. \\ \mathcal{D}_2 &: (y_1, \dots, y_{p-1}, y_p \cos \alpha, y_p \sin \alpha, 0, 0, \dots, 0), & y_p \geq 0.\end{aligned}\quad (2.21)$$

Where now the $(p-1)$ -dimensional mutual edge \mathcal{I} is located at $x_p = y_p = 0$. We also refer to the same action as (2.12), only now with a different defect geometry. As in the previous part, we look at the $\int_{\mathcal{D}_1} \int_{\mathcal{D}_2} \mathcal{O}_i \mathcal{O}_j$ term in (2.15) and perform the OPE around the point $x = (\vec{x}_{p-1}, 0)$,

$$\begin{aligned}\int_{\mathcal{D}_1} \int_{\mathcal{D}_2} \mathcal{O}_i \mathcal{O}_j &= \\ &= \int d^{p-1}x \int d^{p-1}y \int_0^\infty dx_p \int_0^\infty dy_p \frac{C_{ij}^\alpha \mathcal{O}_\alpha(\vec{x}_{p-1}, 0)}{((\vec{x}_{p-1} - \vec{y}_{p-1})^2 + (x_p - y_p \cos \alpha)^2 + y_p^2 \sin^2 \alpha)^{\frac{\Delta_{ij\alpha}}{2}}} + \dots\end{aligned}\quad (2.22)$$

After applying (A.1) we have,

$$\begin{aligned}\int_{\mathcal{D}_1} \int_{\mathcal{D}_2} \mathcal{O}_i \mathcal{O}_j &= \frac{\pi^{\frac{p-1}{2}} \Gamma\left(\frac{\Delta_{ij\alpha} - p + 1}{2}\right)}{\sin \alpha \Gamma\left(\frac{\Delta_{ij\alpha}}{2}\right)} \int d^{p-1}x \int_0^\infty dy_p \frac{C_{ij}^\alpha \mathcal{O}_\alpha(\vec{x}_{p-1}, 0)}{y_p^{\Delta_{ijk} - p + 1}} \times \\ &\times \left[(x_p) {}_2F_1\left(\frac{1}{2}, \frac{\Delta_{ijk} - p + 1}{2}; \frac{3}{2}; \frac{-x_p^2}{y_p^2}\right) \right]_{x_p = -y_p \cot \alpha}^{x_p \rightarrow \infty}\end{aligned}\quad (2.23)$$

Where ${}_2F_1$ is a Hypergeometric function. For the $x_p \rightarrow \infty$ limit, we use the asymptotic expansion,

$$\begin{aligned}(x_p) {}_2F_1\left(\frac{1}{2}, \frac{\Delta_{ijk} - p + 1}{2}; \frac{3}{2}; -\frac{x_p^2}{y_p^2}\right) &= \frac{\sqrt{\pi} \Gamma\left(\frac{\Delta_{ijk} - p}{2}\right) y_p}{2 \Gamma\left(\frac{\Delta_{ijk} - p + 1}{2}\right)} + \mathcal{O}\left(\frac{1}{x_p}\right) \\ &+ \left(\frac{y_p^2}{x_p^2}\right)^{\frac{\Delta_{ijk} - p - 1}{2}} \left[\frac{x_p}{p - 1 - \Delta_{ijk} + 1} + \mathcal{O}\left(\frac{1}{x_p}\right) \right],\end{aligned}\quad (2.24)$$

and take the first term in (2.24).⁵ Together with the lower limit of integration over x_p , we overall have,

$$\int_{\mathcal{D}_1} d^2x \int_{\mathcal{D}_2} d^2y \mathcal{O}_i(x) \mathcal{O}_j(y) = W(\alpha) \int_0^\infty \frac{dy_p}{y_p^{\Delta_{ijk} - p}} \times \int d^{p-1}x C_{ij}^\alpha \mathcal{O}_\alpha(\vec{x}_{p-1}, 0) + \dots \quad (2.25)$$

⁵The second line in (2.24) contributes to non-universal power law divergences.

Where,

$$W(\alpha) = \frac{\pi^{\frac{p-1}{2}} \Gamma\left(\frac{\Delta_{ij\alpha} - p - 1}{2}\right)}{\sin \alpha \Gamma\left(\frac{\Delta_{ij\alpha}}{2}\right)} \left[\frac{\sqrt{\pi} \Gamma\left(\frac{\Delta_{ijk} - p}{2}\right)}{2\Gamma\left(\frac{\Delta_{ijk} - p + 1}{2}\right)} + (\cot \alpha) {}_2F_1\left(\frac{1}{2}, \frac{\Delta_{ij\alpha} - p + 1}{2}; \frac{3}{2}; -\cot^2 \alpha\right) \right]. \quad (2.26)$$

If considering weakly relevant deformations with $\Delta_i = p - \epsilon_i$, $\Delta_\alpha = p - 1 - \epsilon_\alpha$, then (2.26) greatly simplifies with the aid of the identity ${}_2F_1\left(\frac{1}{2}, 1; \frac{3}{2}; -z^2\right) = \frac{\arctan(z)}{z}$, giving,

$$\int_{\mathcal{D}_1} \int_{\mathcal{D}_2} \mathcal{O}_i \mathcal{O}_j = \left(\frac{\pi - \alpha}{\sin \alpha} \frac{\pi^{\frac{p-1}{2}}}{\Gamma\left(\frac{p+1}{2}\right)} \int_{\mu^{-1}}^{\infty} \frac{dy_p}{y_p^{1-\epsilon_{ij\alpha}}} \right) \times \int d^{p-1}x C_{ij}^\alpha \mathcal{O}_\alpha(\vec{x}_{p-1}, 0) + \dots \quad (2.27)$$

As a consistency check, note that the free field cusp anomalous dimension [67] can be retrieved by setting \mathcal{O}_α to be the identity operator (hence $p = 1$). In such case both (2.6), (2.27) sum together to yield the correct result. Combining the above with (2.7) and (2.18), we arrive at the following beta function,

$$\begin{aligned} \beta_\alpha = & -\epsilon_\alpha h_\alpha + \frac{\pi^{\frac{p-1}{2}} C_\alpha^{\beta\gamma}}{\Gamma\left(\frac{p-1}{2}\right)} h_\beta h_\gamma + \frac{\pi^{\frac{p}{2}} C_\alpha^{i\beta}}{\Gamma\left(\frac{p}{2}\right)} \left(g_i^{(1)} + g_i^{(2)} \right) h_\beta \\ & + \frac{\pi^{\frac{p-1}{2}} C_\alpha^{ij}}{\Gamma\left(\frac{p+1}{2}\right)} \left(\frac{\pi - \alpha}{\sin \alpha} g_i^{(1)} g_j^{(2)} - \frac{g_i^{(1)} g_j^{(1)} + g_i^{(2)} g_j^{(2)}}{2} \right). \end{aligned} \quad (2.28)$$

Note that when $g^{(1)}, g^{(2)}$ are identical and $\alpha = \pi$, the last term in (2.28) vanish. Indeed, in this case there is just an infinite plane and the edge disappears.⁶

2.4 Example: $(\phi^4)_{\mathcal{D}_1} \cap (\phi^4)_{\mathcal{D}_2} : (\phi^2)_{\mathcal{I}}$ in Tricritical Bulk

This is a nice tractable example of a perturbative RG flow that can be studied with the tools that were presented. We consider a bulk theory in $d = 3 - \epsilon$ dimensions with N scalar fields that is described by the tricritical model,

$$S_{\text{bulk}} = \int d^{3-\epsilon}x \left(\frac{1}{2} (\partial\phi)^2 + \lambda (\phi^2)^3 \right). \quad (2.29)$$

The operators ϕ^2 and ϕ^4 have dimensions close to and 1 and 2 respectively, and are hence available for constructing the different geometric objects studied above. The bulk coupling has the following beta function to leading order in epsilon [94, 95],

$$\beta_\lambda = -2\epsilon\lambda + \frac{3(3N + 22)}{\pi^2} \lambda^2. \quad (2.30)$$

⁶More exactly, if $h_\alpha = 0$ it will remain so. It is possible to start with a non vanishing h_α that will flow to a non-trivial fixed-point. That would describe a composite defect [92, 93].

At the IR fixed point $\lambda^* = \frac{2\pi^2\epsilon}{3(3N+22)}$, the operators ϕ^2 and ϕ^4 assume the following anomalous dimensions,

$$\gamma_{\phi^4} = -\frac{4(N+4)}{3N+22}\epsilon, \quad (2.31)$$

$$\gamma_{\phi^2} = -\frac{5(N+2)(N+4)}{4(3N+22)^2}\epsilon^2. \quad (2.32)$$

To utilize conformal perturbation theory in what follows, we use the following data,

$$C_{\phi^2}^{\phi^2\phi^2} = 4C_\phi, \quad C_{\phi^2}^{\phi^4\phi^2} = 4(N+2)C_\phi^2, \quad C_{\phi^2}^{\phi^4\phi^4} = 32(N+2)C_\phi^3 \quad (2.33)$$

$$C_{\phi^4}^{\phi^4\phi^4} = 8(N+8)C_\phi^2, \quad C_\phi = \frac{\Gamma\left(\frac{d-2}{2}\right)}{4\pi^{\frac{d}{2}}}.$$

Semi-Infinite Plane

This case is described by the action,

$$S = S_{\text{bulk}} + g_0 \int_{\mathcal{D}} d^p x \phi^4 + h_0 \int_{\delta\mathcal{D}} d^{p-1} x \phi^2, \quad (2.34)$$

Where the bulk is fixed in dimension $d = 3 - \epsilon$ and controlled by action (2.29). We can consider (at least) two different models, which are both interesting on their own. One is for $p = 2$ and the second is for $p = 2 - \epsilon$. We shall inspect both of them. The beta functions are obtained from (2.8),(2.9) and (2.33),

$$\beta_g = -(p - \Delta_{\phi^4})g + (N+8)\frac{g^2}{2\pi}, \quad (2.35)$$

$$\beta_h = -(p-1 - \Delta_{\phi^2})h + \frac{h^2}{\pi} + \frac{N+2}{4}\frac{gh}{\pi} - \frac{N+2}{2}\frac{g^2}{\pi^3}. \quad (2.36)$$

Where $\Delta_{\phi^4} = 2 - 2\epsilon$, $\Delta_{\phi^2} = 1 - \epsilon$ for non-interacting bulk, and when the bulk is critical at $\lambda = \lambda^*$ these are added with the anomalous dimensions (2.31),(2.32).⁷ We now explore the various possibilities,⁸

- $p = 2$, $\lambda = 0$:

$$g^* = \frac{4\pi\epsilon}{N+8}, \quad h_{\pm}^* = \frac{3\pi\epsilon}{N+8} \pm \frac{\pi}{2}\gamma_{e,1}, \quad (2.37)$$

$$\gamma_{e,1} = \frac{6\epsilon}{N+8} \sqrt{1 + 8\frac{N+2}{(3\pi)^2}}. \quad (2.38)$$

⁷The anomalous dimension (2.32) is order $\mathcal{O}(\epsilon^2)$, so does not contribute to the leading order in ϵ .

⁸For a non-interacting bulk ($\lambda = 0$), a related model of a composite defect (1d ϕ^2 defect inside a 2d ϕ^4 defect) was studied in [93]. We indeed verified that our results for $\lambda = 0, p = 2$ are consistent with their findings, up to the appropriate factors explained in the previous section.

- $p = 2 - \epsilon$, $\lambda = 0$:

$$g^* = \frac{2\pi\epsilon}{(N+8)}, \quad h_{\pm}^* = -\frac{N+2}{N+8} \frac{\pi\epsilon}{4} \pm \frac{\pi}{2} \gamma_{e,2}, \quad (2.39)$$

$$\gamma_{e,2} = \frac{N+2}{N+8} \frac{\epsilon}{2} \sqrt{1 + \frac{32}{\pi^2 (N+2)}}. \quad (2.40)$$

- $p = 2$, $\lambda = \lambda^*$:

$$g^* = \frac{20(N+6)}{(3N+22)(N+8)} \pi\epsilon, \quad (2.41)$$

$$h_{\pm}^* = -\frac{(N^2 - 3N - 58)\pi\epsilon}{(3N+22)(N+8)} \pm \frac{\pi}{2} \gamma_{e,3}, \quad (2.42)$$

$$\gamma_{e,3} = \frac{2(N^2 - 3N - 58)\epsilon}{(3N+22)(N+8)} \sqrt{1 + \frac{200(N+2)(N+6)^2}{\pi^2 (N^2 - 3N - 58)^2}}. \quad (2.43)$$

- $p = 2 - \epsilon$, $\lambda = \lambda^*$:

$$g^* = \frac{7N+38}{(3N+22)(N+8)} \pi\epsilon, \quad (2.44)$$

$$h_{\pm}^* = -\frac{(7N+38)(N+2)\pi\epsilon}{8(3N+22)(N+8)} \pm \frac{\pi}{2} \gamma_{e,4}, \quad (2.45)$$

$$\gamma_{e,4} = \frac{(7N+38)(N+2)\epsilon}{4(3N+22)(N+8)} \sqrt{1 + \frac{32}{\pi^2 (N+2)}}. \quad (2.46)$$

In all cases the discriminant is positive for all N . The flow takes its course from the UV fixed-point h_-^* to the IR fixed-point h_+^* . By shifting the coupling constant to $\tilde{h} = h - h_-^*$, the beta function (2.36) takes the form,

$$\beta_{\tilde{h}} = -\gamma_e \tilde{h} + \frac{\tilde{h}^2}{\pi}. \quad (2.47)$$

The interpretation of (2.47) is simple - the flow begins at the UV from a non-trivial weakly coupled "Edge-CFT", deformed by a slightly relevant edge deformation with dimension $\Delta = p + \gamma_e$ and terminating at the IR fixed-point with $\tilde{h}^* = h_+^* - h_-^*$.

Two Intersecting Planes

We use the following action,

$$S = S_{\text{bulk}} + g_0^{(1)} \int_{\mathcal{D}_1} d^p x \phi^4 + g_0^{(2)} \int_{\mathcal{D}_2} d^p x \phi^4 + h_0 \int_{\mathcal{I}} d^{p-1} x \phi^2. \quad (2.48)$$

The beta functions are obtained from (2.19),(2.20) and (2.33). In this case $g^{(1)} = g^{(2)}$ and we simply call both of these couplings g . Therefore,

$$\beta_g = -(p - \Delta_{\phi^4})g + (N + 8) \frac{g^2}{2\pi}, \quad (2.49)$$

$$\beta_h = -(p - 1 - \Delta_{\phi^2})h + \frac{h^2}{\pi} + (N + 2) \frac{gh}{\pi} + (N + 2) \frac{g^2}{\pi^2 \sin \alpha}. \quad (2.50)$$

We list the four different possibilities,

- $p = 2, \lambda = 0, g^* = \frac{4\pi\epsilon}{N+8}$:

$$h_{\pm}^* = -\frac{N - 4}{N + 8} \frac{\pi\epsilon}{2} \pm \frac{\pi}{2} \gamma_{i,1}(\alpha), \quad (2.51)$$

$$\gamma_{i,1}(\alpha) = \frac{N - 4}{N + 8} \epsilon \sqrt{1 - \frac{32(N + 2)}{\pi(N - 4)^2 \sin \alpha}}. \quad (2.52)$$

- $p = 2 - \epsilon, \lambda = 0, g^* = \frac{2\pi\epsilon}{(N+8)}$:

$$h_{\pm}^* = -\frac{N + 2}{N + 8} \pi\epsilon \pm \frac{\pi}{2} \gamma_{i,2}(\alpha), \quad (2.53)$$

$$\gamma_{i,2}(\alpha) = 2 \frac{N + 2}{N + 8} \epsilon \sqrt{1 - \frac{8}{\pi(N + 2) \sin \alpha}}. \quad (2.54)$$

- $p = 2, \lambda = \lambda^*, g^* = \frac{20(N+6)}{(3N+22)(N+8)} \pi\epsilon$:

$$h_{\pm}^* = -\frac{(17N^2 + 114N + 64) \pi\epsilon}{2(N + 8)(3N + 22)} \pm \frac{\pi}{2} \gamma_{i,3}(\alpha), \quad (2.55)$$

$$\gamma_{i,3}(\alpha) = \frac{(17N^2 + 114N + 64) \epsilon}{(N + 8)(3N + 22)} \sqrt{1 - \frac{3200(N + 2)(N + 6)^2}{\pi(17N^2 + 114N + 64)^2 \sin \alpha}}. \quad (2.56)$$

- $p = 2 - \epsilon, \lambda = \lambda^*, g^* = \frac{7N+38}{(3N+22)(N+8)} \pi\epsilon$:

$$h_{\pm}^* = -\frac{\pi(N + 2)(7N + 38) \epsilon}{2(N + 8)(3N + 22)} \pm \frac{\pi}{2} \gamma_{i,4}(\alpha), \quad (2.57)$$

$$\gamma_{i,4}(\alpha) = \frac{(N + 2)(7N + 38) \epsilon}{(N + 8)(3N + 22)} \sqrt{1 - \frac{8}{\pi(N + 2) \sin \alpha}}. \quad (2.58)$$

As the intersection angle is gradually decreased, a putative critical angle appears when $\gamma_i(\alpha_c) = 0$. We note that this behavior was also observed in [47, 52] (see also comment in [54]). At this level of computation, we can not determine if this indicates an actual physical phenomenon or whether this is an artifact of perturbation theory. The latter is definitely plausible, as for when $\gamma_i = 0$ one must resort to the next order in perturbation theory.

Wedge Formed by Two Semi-Infinite planes

This is a modification of the above, where the beta functions are obtained from (2.20), (2.28) and (2.33). In this case $g^{(1)} = g^{(2)}$ and we simply call both of these couplings g ,

$$\beta_g = -(p - \Delta_{\phi^4})g + (N + 8) \frac{g^2}{2\pi}, \quad (2.59)$$

$$\beta_h = -(p - 1 - \Delta_{\phi^2})h + \frac{h^2}{\pi} + (N + 2) \frac{gh}{2\pi} + (N + 2) W(\alpha) \frac{g^2}{\pi^3}. \quad (2.60)$$

Where,

$$W(\alpha) = \frac{\pi - \alpha}{\sin(\alpha)} - 1. \quad (2.61)$$

The four cases are then tabulated as,

- $p = 2, \lambda = 0, g^* = \frac{4\pi\epsilon}{N+8}$:

$$h_{\pm}^* = -\frac{N - 4}{N + 8} \frac{\pi\epsilon}{2} \pm \frac{\pi}{2} \gamma_{w,1}(\alpha), \quad (2.62)$$

$$\gamma_{w,1}(\alpha) = \frac{N - 4}{N + 8} \epsilon \sqrt{1 - \frac{64(N + 2)}{\pi^2(N - 4)^2} W(\alpha)}. \quad (2.63)$$

- $p = 2 - \epsilon, \lambda = 0, g^* = \frac{2\pi\epsilon}{(N+8)}$:

$$h_{\pm}^* = -\frac{N + 2}{N + 8} \frac{\pi\epsilon}{2} \pm \frac{\pi}{2} \gamma_{w,2}(\alpha), \quad (2.64)$$

$$\gamma_{w,2}(\alpha) = \frac{N + 2}{N + 8} \epsilon \sqrt{1 - \frac{16W(\alpha)}{\pi^2(N + 2)}}. \quad (2.65)$$

- $p = 2, \lambda = \lambda^*, g^* = \frac{20(N+6)}{(3N+22)(N+8)}\pi\epsilon$:

$$h_{\pm}^* = -\frac{7N^2 + 34N - 56}{(N + 8)(3N + 22)} \frac{\pi\epsilon}{2} \pm \frac{\pi}{2} \gamma_{w,3}(\alpha), \quad (2.66)$$

$$\gamma_{w,3}(\alpha) = \frac{7N^2 + 34N - 56}{(N + 8)(3N + 22)} \epsilon \sqrt{1 - \frac{1600(N + 2)(N + 6)^2 W(\alpha)}{\pi^2(7N^2 + 34N - 56)^2}}. \quad (2.67)$$

- $p = 2 - \epsilon$, $\lambda = \lambda^*$, $g^* = \frac{7N+38}{(3N+22)(N+8)}\pi\epsilon$:

$$h_{\pm}^* = -\frac{(N+2)(7N+38)}{(N+8)(3N+22)}\frac{\pi\epsilon}{4} \pm \frac{\pi}{2}\gamma_{w,4}(\alpha), \quad (2.68)$$

$$\gamma_{w,4}(\alpha) = \frac{(N+2)(7N+38)}{(N+8)(3N+22)}\frac{\epsilon}{2}\sqrt{1 - \frac{16W(\alpha)}{\pi^2(N+2)}}. \quad (2.69)$$

Just like for the two intersecting planes discussed previously, the issue of the putative critical angle that appears as α is decreased remains here as well. The $\alpha = \pi$ case gives the values for the composite line defect.

3 Three Defects: Trihedral & 3-Line Corners

We may also explore the possibility of the emergence of degrees of freedom taking place at the mutual intersection of more than two defects. In contrast to two defects nevertheless, novel terms in the beta function such as the one appearing in (2.19) begin from cubic order (for 3 defects for instance, there would be a term in the beta function $\propto g^{(1)}g^{(2)}g^{(3)}$) and hence fall beyond the scope of conformal perturbation theory. A notable exception however in when conformal perturbation can be applied beyond two defects is when the mutual intersection is a point.

The minimal number of p -dimensional planes that are required to mutually intersect at a point is $p+1$. Indeed, the simplest object of this kind is a cusp formed by two lines ($p = 1$), presenting itself in the free energy as a logarithmic term known as the cusp anomalous dimension [67, 86, 87]. Furthermore, we may consider three 2-dimensional planes intersecting at a point ($p = 2$), an object that we refer to as a Trihedral Corner. It will give rise to an anomalous dimension through a novel logarithmic term appearing in the free energy that is remarkably still accessible by conformal perturbation theory at the level of the three-point function.

3.1 Trihedral Corners

To study the trihedral corner anomaly, consider three 2-dimensional planar defects in $\mathbb{R}^{d \geq 3}$: $\mathcal{D}_1, \mathcal{D}_2, \mathcal{D}_3$, as they are described by the action,

$$S = S_{\text{CFT}} + \sum_{a=1}^3 g_i^{(a)} \int_{\mathcal{D}_a} d^2x \mathcal{O}_i. \quad (3.1)$$

As a lesson from the last section, we should also account for the fact that three line defects will possibly be generated at the intersection of each pair of planes. It is important

to emphasize that this effect is not directly related to the trihedral corner anomaly, but it is interesting on its own regardless, and its ramifications will be separately discussed in part 3.2. For the computation of the anomaly coefficient we assume that $\Delta_i = 2$, although the result is also applicable for slightly relevant deformations. The corner anomalous dimension $\Gamma_{\text{trihedral}}$ will arise from the following term in the free energy,⁹

$$\begin{aligned} \log Z &= -\Gamma_{\text{trihedral}} \log \left(\frac{L}{a} \right) + \dots \\ &= -g_i^{(1)} g_j^{(2)} g_k^{(3)} \int_{\mathcal{D}_1} d^2x \int_{\mathcal{D}_2} d^2y \int_{\mathcal{D}_3} d^2z \langle \mathcal{O}_i(x) \mathcal{O}_j(y) \mathcal{O}_k(z) \rangle + \dots \end{aligned} \quad (3.2)$$

We define the three unit vectors \hat{e}_1, \hat{e}_2 and \hat{e}_3 such that they lay parallel to the edges of intersection $\mathcal{I}_{13}, \mathcal{I}_{12}, \mathcal{I}_{23}$ respectively (see Fig. 3). The vectors are used to parameterize the three planes by,

$$\mathcal{D}_1(x_1, x_2) = x_1 \hat{e}_1 + x_2 \hat{e}_2, \quad \mathcal{D}_2(y_1, y_2) = y_1 \hat{e}_2 + y_2 \hat{e}_3, \quad \mathcal{D}_3(z_1, z_2) = z_1 \hat{e}_3 + z_2 \hat{e}_1. \quad (3.3)$$

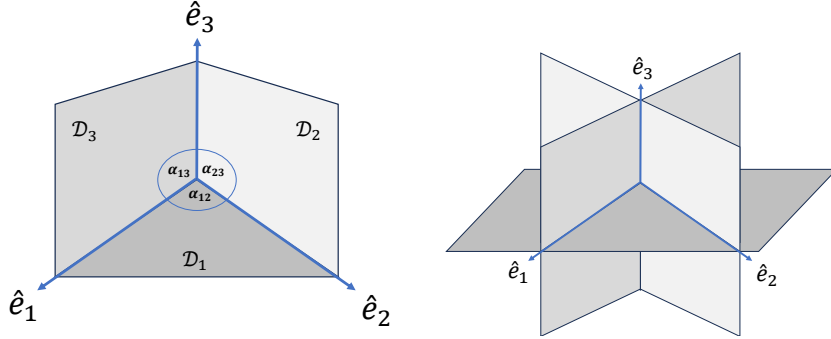


Figure 3. *Left:* A trihedral corner subtended by the three unit vectors $\hat{e}_1, \hat{e}_2, \hat{e}_3$. The relative angles $\hat{e}_a \cdot \hat{e}_b = \cos(\alpha_{ab})$ are also drawn. *Right:* An extended trihedral corner.

There are (at least) two geometric objects that we may consider. The first object is literally a corner. This is the 3 defect analog of the wedge 2.3 and it is parameterized by requiring that all parameters x_1, x_2, \dots, z_2 in (3.3) be positive. More accurately, it is the boundary of the polyhedral convex cone generated by $\hat{e}_1, \hat{e}_2, \hat{e}_3$.

The second geometric object is an extended corner. This is the analog of 2.2 and can be considered as the gluing of eight corners. To put it differently, all three planes extend indefinitely, with all the parameters in (3.3) unrestricted other than being real. We

⁹ L and a are IR and UV regulators respectively. L can be thought of as the size of the defects.

shall perform the computation for the extended trihedral corner, where the second case is left for a future study.¹⁰ For that end we write the integrated three-point function (3.2) explicitly by using parameterization (3.3),

$$\int_{\mathcal{D}_1} \int_{\mathcal{D}_2} \int_{\mathcal{D}_3} \langle \mathcal{O}_i \mathcal{O}_j \mathcal{O}_k \rangle = C_{ijk} \int d^2x \int d^2y \int d^2z \frac{\sin(\alpha_{12}) \sin(\alpha_{23}) \sin(\alpha_{13})}{|x-y|^2 |x-z|^2 |z-y|^2}, \quad (3.4)$$

$$\begin{aligned} |x-y|^2 &= x_1^2 + y_2^2 + (x_2 - y_1)^2 + 2y_2 \cos(\alpha_{23})(y_1 - x_2) \\ &\quad + 2x_1 (\cos(\alpha_{12})(x_2 - y_1) - y_2 \cos(\alpha_{13})). \end{aligned} \quad (3.5)$$

Where the other distances in (3.4) are obtained from permutations of (3.5). Next we perform Feynman parameterization (A.2) and define the vector $X = (x_1, x_2, y_1, y_2, z_1, z_2)$. As so, the integral inside (3.4) can be expressed as,

$$\iiint \frac{d^2x d^2y d^2z}{|x-y|^2 |x-z|^2 |z-y|^2} = 2 \int_0^1 du \int_0^1 dv (1-v) \int \frac{d^6X}{(X^T M X)^6}, \quad (3.6)$$

Where M is a (6×6) real symmetric matrix with coefficients depending on u, v and $\alpha_{12}, \alpha_{23}, \alpha_{13}$. We diagonalize by change of variables,

$$\iiint \frac{d^2x d^2y d^2z}{|x-y|^2 |x-z|^2 |z-y|^2} = 2\pi^3 \int_0^1 du \int_0^1 dv \frac{1-v}{(\det M(u, v))^{1/2}} \int \frac{dX}{X}, \quad (3.7)$$

Remarkably, the determinant factorizes to,

$$\begin{aligned} \det M &= (1-v)^3 (u(1-u)(1-v) + v)^3 \times V^4(\alpha_{12}, \alpha_{23}, \alpha_{13}), \\ V^2(\alpha_{12}, \alpha_{23}, \alpha_{13}) &= 1 + 2 \cos(\alpha_{12}) \cos(\alpha_{13}) \cos(\alpha_{23}) - \cos^2(\alpha_{12}) - \cos^2(\alpha_{13}) - \cos^2(\alpha_{23}). \end{aligned} \quad (3.8)$$

Where $V(\alpha_{12}, \alpha_{23}, \alpha_{13}) = |\hat{e}_1 \wedge \hat{e}_2 \wedge \hat{e}_3|$ is the volume of the unit Parallelepiped subtended by $\hat{e}_1, \hat{e}_2, \hat{e}_3$. The integrals over u, v can then be carried out straightforwardly and one finds,

$$\iiint \frac{d^2x d^2y d^2z}{|x-y|^2 |x-z|^2 |z-y|^2} = \frac{4\pi^4}{V^2(\alpha_{12}, \alpha_{23}, \alpha_{13})} \int \frac{dX}{X}. \quad (3.9)$$

¹⁰The structure of the non-extend corner is more involved. This is because every single face of the trihedron has a corner independently, and therefore preceding (3.2) there will be logarithmic contributions already appearing at the level of the two-point function.

In conclusion,

$$\Gamma_{\text{ext.-trihedral}}(\alpha_{12}, \alpha_{23}, \alpha_{13}) = \frac{\sin(\alpha_{12}) \sin(\alpha_{23}) \sin(\alpha_{13})}{V^2(\alpha_{12}, \alpha_{23}, \alpha_{13})} 4\pi^4 C^{ijk} g_i^{(1)} g_j^{(2)} g_k^{(3)}. \quad (3.10)$$

As expected, (3.10) is symmetric with respect to $\alpha_{12}, \alpha_{23}, \alpha_{13}$ and diverges when $\hat{e}_1, \hat{e}_2, \hat{e}_3$ are co-planar, meaning an overlap between the planes. Furthermore, a special case that is worth mentioning is when two angles are equal to $\frac{\pi}{2}$ and the remaining one to α ,

$$\Gamma_{\text{ext.-trihedral}}(\alpha) = \frac{4\pi^4}{\sin \alpha} C^{ijk} g_i^{(1)} g_j^{(2)} g_k^{(3)}, \quad (3.11)$$

Note that this functional dependence on α is identical to the one appearing in the anomalous dimension of two intersecting lines (3.16).

3.2 The 3-Line Potential

Another interesting related object is a 3-line corner, composed of three mutually intersecting line defects in $\mathbb{R}^{d \geq 3}$ (see Fig. 4).¹¹ It stands both on its own and as an emergent object that can appear at the edges of trihedral corners. As before, the action is,¹²

$$S = S_{\text{CFT}} + \sum_{a=1}^3 h_a \int_{\mathcal{D}_a} dx \mathcal{O}_a. \quad (3.12)$$

Where we assume that $\Delta_a = 1$, only for performing the computation. The three line defects are pointing at the directions defined by the unit vectors,

$$\mathcal{D}_1(x) = x\hat{e}_1, \mathcal{D}_2(y) = y\hat{e}_2, \mathcal{D}_3(z) = z\hat{e}_3. \quad (3.13)$$

There will be several terms appearing in the anomaly coefficient,

$$\Gamma = \sum_{a < b}^3 \Gamma_{\text{cusp}}(\alpha_{ab}) + \Gamma_{\text{3-line}}(\alpha_{12}, \alpha_{23}, \alpha_{13}). \quad (3.14)$$

The well-known cusp terms arise at the level of the second order/two-point function in the free energy and are given by [67],

$$\Gamma_{\text{cusp}}(\alpha_{ab}) = -\frac{\pi - \alpha_{ab}}{\sin(\alpha_{ab})} h_a h_b + \frac{h_a^2 + h_b^2}{2}, \quad (3.15)$$

¹¹Corners/star-shaped configurations with n-lines were studied in [45] for $d = 2$.

¹²In this case, to avoid proliferation of indices we assume just a single deformation on each line. Generalization to multiple deformations is straightforward.

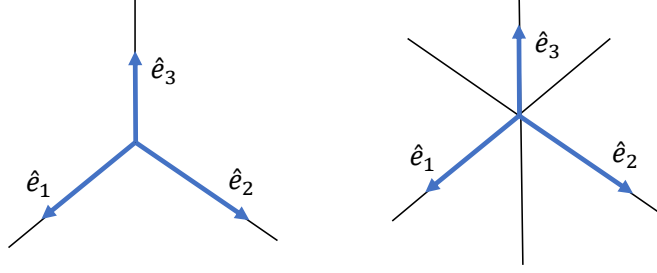


Figure 4. *Left:* A 3-line corner defined with $\hat{e}_1, \hat{e}_2, \hat{e}_3$ and parameterized by $x, y, z \geq 0$. *Right:* An extended 3-line corner, parameterized by $x, y, z \in \mathbb{R}$. Relative angles are defined by $\hat{e}_a \cdot \hat{e}_b = \cos(\alpha_{ab})$.

In case the cusp is extended (2 intersecting infinite lines), one can obtain the anomalous dimension by direct calculation such as in (2.17) or alternatively by gluing together 4 cusps with supplementary angles α and $\pi - \alpha$,

$$\Gamma_{2\text{-lines}}(\alpha_{ab}) = -\frac{2\pi}{\sin(\alpha_{ab})} h_a h_b. \quad (3.16)$$

The focus of this subsection is $\Gamma_{3\text{-line}}$, arising from all three lines meeting mutually at a single point. There are two cases that can be studied, as depicted in Fig. 4. For the 3-line corner, we may view each line as the world-line of a point-like impurity via conformal mapping to the cylinder [45, 67]. In this interpretation one can think of $\Gamma_{3\text{-line}}$ as the three-body potential of impurities living on S^{d-1} . We shall derive this potential for the two cases by computing the following term in the free energy,

$$\begin{aligned} \log Z &= -\Gamma_{3\text{-line}}(\alpha_{12}, \alpha_{23}, \alpha_{13}) \log\left(\frac{L}{a}\right) + \dots \\ &= -h_1 h_2 h_3 \int_{\mathcal{D}_1} dx \int_{\mathcal{D}_2} dy \int_{\mathcal{D}_3} dz \langle \mathcal{O}_1(x) \mathcal{O}_2(y) \mathcal{O}_3(z) \rangle + \dots \end{aligned} \quad (3.17)$$

For that task we have to address the following integral,

$$\iiint \frac{dx dy dz}{\sqrt{(x^2 + y^2 - 2xy \cos \alpha_{12})} \sqrt{(x^2 + z^2 - 2xz \cos \alpha_{13})} \sqrt{(y^2 + z^2 - 2yz \cos \alpha_{23})}}, \quad (3.18)$$

Where the range of integration for the non-extended 3-line corner is over the domain $x, y, z \geq 0$. By moving to cylindrical coordinates (z, ρ, θ) and rescaling z to a dimen-

sionless variable $z = t\rho$, we rewrite the integral (3.18) as $\mathcal{J}(\alpha_{12}, \alpha_{23}, \alpha_{13}) \int \frac{d\rho}{\rho}$, where,

$$\mathcal{J}_{\frac{\pi}{2}}(\alpha_{12}, \alpha_{23}, \alpha_{13}) = \int_0^{\pi/2} d\theta \frac{I_{\alpha_{13}, \alpha_{23}}(\theta)}{\sqrt{(1 - \cos \alpha_{12} \sin 2\theta)}}, \quad (3.19)$$

$$\mathcal{J}_{2\pi}(\alpha_{12}, \alpha_{23}, \alpha_{13}) = \int_0^{2\pi} d\theta \frac{I_{\alpha_{13}, \alpha_{23}}(\theta) + I_{\pi - \alpha_{13}, \pi - \alpha_{23}}(\theta)}{\sqrt{(1 - \cos \alpha_{12} \sin 2\theta)}}, \quad (3.20)$$

And $I_{\alpha, \beta}(\theta)$ is the following elliptic integral,

$$I_{\alpha, \beta}(\theta) = \int_0^{\infty} \frac{dt}{\sqrt{((t - \cos \alpha \cos \theta)^2 + \sin^2 \alpha \cos^2 \theta) ((t - \cos \beta \sin \theta)^2 + \sin^2 \beta \sin^2 \theta)}}. \quad (3.21)$$

$\mathcal{J}_{\frac{\pi}{2}}$ is used for the 3-line corner, and $\mathcal{J}_{2\pi}$ for the extended one. The integral (3.21) has a closed form solution that is fully described in (A.3). In conclusion,

$$\Gamma_{\text{3-line}}(\alpha_{12}, \alpha_{23}, \alpha_{13}) = Ch_1 h_2 h_3 \mathcal{J}_{\frac{\pi}{2}}(\alpha_{12}, \alpha_{23}, \alpha_{13}), \quad (3.22)$$

$$\Gamma_{\text{ext.-3-line}}(\alpha_{12}, \alpha_{23}, \alpha_{13}) = Ch_1 h_2 h_3 \mathcal{J}_{2\pi}(\alpha_{12}, \alpha_{23}, \alpha_{13}). \quad (3.23)$$

Where C is the OPE coefficient. For the purpose of demonstration, it is enough to consider the case, $\alpha_{23} = \alpha_{13} = \frac{\pi}{2}$, $\alpha_{12} = \alpha$, because (3.21) simplifies considerably,¹³

$$I_{\frac{\pi}{2}, \frac{\pi}{2}}(\theta) = \frac{K(1 - \cot^2 \theta)}{|\sin \theta|}, \quad (3.24)$$

Where K is the Complete Elliptic Integral of the First Kind (A.4).

\mathcal{J} can be computed numerically, as demonstrated in Fig. 5. We observe that $\mathcal{J}_{\frac{\pi}{2}}(\alpha \rightarrow \pi)$ approaches a non-vanishing value, which is also a minimum due to the reflection symmetry, $\mathcal{J}_{\frac{\pi}{2}}(\alpha) = \mathcal{J}_{\frac{\pi}{2}}(2\pi - \alpha)$. This value is related to the non-vanishing Casimir energy of the "T"-shape configuration the 3 line defects assume at $\alpha = \pi$. For the extended corner, the $\alpha \rightarrow \pi - \alpha$ symmetry is clearly viewable. Finally, notice that as $\alpha \rightarrow 0$ the 3-line potential has the form of $\Gamma_{\text{3-line}}(\alpha) \approx c_1 \log \alpha + c_2$. This fact is consistent with the notion of fusions of line defects [64, 67], as when $\alpha_{12} \rightarrow 0$, the full potential (3.14) should relate to a single cusp that is formed by \mathcal{D}_3 and the fusion product of \mathcal{D}_1 and \mathcal{D}_2 . The $\log \alpha$ term is associated with a slightly irrelevant operator supported on the fused line.

¹³The choice of angles is only a matter of convenience. The result is symmetric in $\alpha_{12}, \alpha_{23}, \alpha_{13}$, as clearly visible in (3.18).

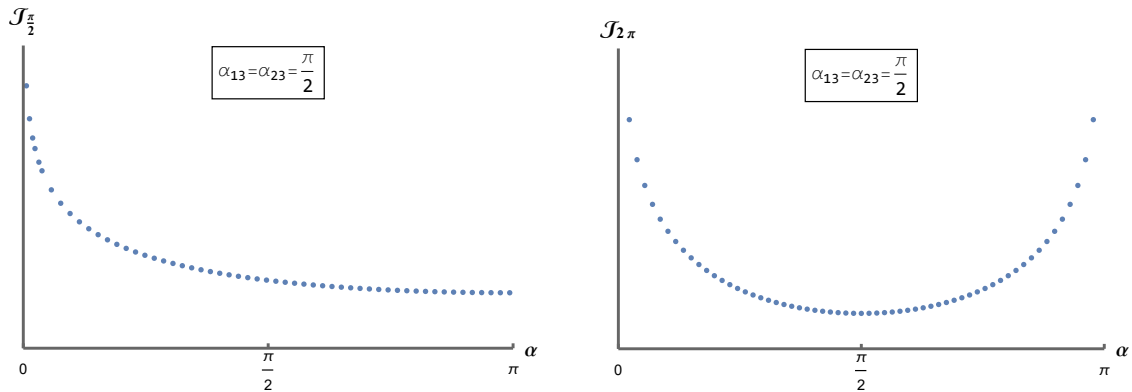


Figure 5. A configuration of 3 line defects with two right angles and $\alpha_{12} = \alpha$ (arbitrarily chosen). *Left Panel:* $\mathcal{J}_{\frac{\pi}{2}}(\alpha)$ Plotted for the 3-line corner. *Right Panel:* $\mathcal{J}_{2\pi}(\alpha)$ Plotted for the extended 3-line corner.

4 Discussion

In the $d = 3 - \epsilon$ tricritical model, we have seen how the operator ϕ^2 is turned on perturbatively at the edges of the ϕ^4 defects. We computed the anomalous dimension of the edge operator for a variety of cases, finding a non-trivial dependence on the angle of intersection α . It is important to understand how the interactions turned on at the edge affect physical observables such as critical exponents. Critical exponents related to the bulk propagator typically display an angular dependence that is linear in $\frac{\pi}{\alpha}$ to leading order [47–58, 61]. They were computed primarily in theories where the wedge sets as the boundary of the bulk, usually specified by Dirichlet and or Neumann conditions. As a first step in understanding critical exponents in systems with intersecting defects, it will be wise to study the $O(N)$ model in $d = 4 - \epsilon$ with wedges composed of localized ϕ^2 interactions [6–10]. I plan to pursue this direction in the future.

It will also be interesting to expand the findings of this paper to deformations involving fermionic and higher-spin primary operators, especially for the 3-line corner that can also be constructed with vector primaries. There is much more left to understand about both the 3-line and trihedral corners. For start, it is intriguing that the cusp anomalous dimension and the 3-line potential have opposite signs. There is hence a very rich structure for the total potential left to be explored for more concrete models. A further curious observation is that the corner anomaly of 2 intersecting lines (3.16) (or extended cusp) and of extended trihedral corners (3.10) have a similar mathematical structure. The structure is clearly related to the inverse volume of the unit Parallelepiped subtended by the corner. It will be interesting to understand if this

pattern persists for higher-dimensional corners involving more than 3 defects, particularly because in that case the anomaly is already related to four-point functions and higher of the bulk CFT.

Acknowledgments

I would like to thank Michael Smolkin, Zohar Komargodski, Ritam Sinha, Gabriel Cuomo, and Barak Kol for the helpful discussions and comments. The work of T.S. is supported by the Israeli Science Foundation Center of Excellence (grant No. 2289/18).

A List of Integrals

Formulas (A.1),(A.2) appear in most QFT textbooks (see *e.g.* [96]). Formula (A.3) is taken from [97].

$$\int d^d x \frac{(x^2)^a}{(x^2 + D)^b} = \pi^{\frac{d}{2}} \frac{\Gamma(b - a - \frac{d}{2}) \Gamma(a + \frac{d}{2})}{\Gamma(b) \Gamma(\frac{d}{2})} \frac{1}{D^{b-a-\frac{d}{2}}}. \quad (\text{A.1})$$

$$\frac{1}{A_1^{\alpha_1} A_2^{\alpha_2} A_3^{\alpha_3}} = \frac{\Gamma(\alpha_1 + \alpha_2 + \alpha_3)}{\Gamma(\alpha_1) \Gamma(\alpha_2) \Gamma(\alpha_3)} \int_0^1 du \int_0^1 dv \frac{u^{\alpha_1-1} (1-u)^{\alpha_2-1} v^{\alpha_3-1} (1-v)^{\alpha_1+\alpha_2-1}}{[(1-v)(uA_1 + (1-u)A_2) + vA_3]^{\alpha_1+\alpha_2+\alpha_3}}. \quad (\text{A.2})$$

$$I(\gamma) = \int_{\gamma_1}^{\gamma} \frac{dt}{\sqrt{((t-b_1)^2 + a_1^2)((t-b_2)^2 + a_2^2)}} = gF(\varphi, k), \quad (\text{A.3})$$

Where in (A.3), g and γ_1 are parameters and $F(\varphi, k)$ is the Incomplete Elliptic Integral of the First Kind with modular angle φ and parameter k (the complete elliptic integral is defined by $K(k) = F(\frac{\pi}{2}, k)$). All are given by,

$$F(\varphi, k) = \int_0^{\varphi} \frac{d\theta}{\sqrt{1 - k^2 \sin^2 \theta}}, \quad (\text{A.4})$$

$$A = \sqrt{(b_1 - b_2)^2 + (a_1 + a_2)^2}, \quad B = \sqrt{(b_1 - b_2)^2 + (a_1 - a_2)^2},$$

$$k^2 = \frac{4AB}{(A+B)^2}, \quad g = \frac{2}{A+B},$$

$$g_1^2 = \frac{4a_1^2 - (A-B)^2}{(A+B)^2 - 4a_1^2}, \quad \gamma_1 = b_1 - a_1 g_1, \quad \tan \varphi = \frac{\gamma - \gamma_1}{a_1 + g_1 b_1 - g_1 \gamma}.$$

Notice that there is a discontinuity when the denominator of $\tan \varphi$ vanishes, and the modular angle jumps from $\frac{\pi}{2}$ to $-\frac{\pi}{2}$. The solution (A.3) remains valid after γ crosses that point if one adds the discontinuity by hand to the integral. For example,

$$\int_0^{\infty} \frac{dt}{\sqrt{((t-b_1)^2+a_1^2)((t-b_2)^2+a_2^2)}} = gF(\varphi(\gamma \rightarrow \infty), k) - gF(\varphi(0), k) + 2gK(k). \quad (\text{A.5})$$

References

- [1] M. Billò, V. Gonçalves, E. Lauria, and M. Meineri, “Defects in conformal field theory,” *Journal of High Energy Physics* **2016** no. 4, (2016) 91.
- [2] S. Liu, H. Shapourian, A. Vishwanath, and M. A. Metlitski, “Magnetic impurities at quantum critical points: Large- N expansion and connections to symmetry-protected topological states,” *Phys. Rev. B* **104** (Sep, 2021) 104201.
- [3] A. Krishnan and M. A. Metlitski, “A plane defect in the 3d $O(N)$ model,” *SciPost Phys.* **15** (2023) 090.
- [4] M. Beccaria, S. Giombi, and A. A. Tseytlin, “Wilson loop in general representation and RG flow in 1D defect QFT,” *Journal of Physics A: Mathematical and Theoretical* **55** no. 25, (Jun, 2022) 255401.
- [5] S. Giombi, E. Helfenberger, and H. Khanchandani, “Line defects in fermionic CFTs,” *Journal of High Energy Physics* **2023** no. 8, (2023) 224.
- [6] S. Giombi and B. Liu, “Notes on a surface defect in the $O(N)$ model,” *Journal of High Energy Physics* **2023** no. 12, (2023) 4.
- [7] T. Shachar, R. Sinha, and M. Smolkin, “RG flows on two-dimensional spherical defects,” *SciPost Phys.* **15** (2023) 240.
- [8] T. Shachar, R. Sinha, and M. Smolkin, “The defect b-theorem under bulk RG flows,” *Journal of High Energy Physics* **2024** no. 9, (2024) 57.
- [9] M. Trépanier, “Surface defects in the $O(N)$ model,” *Journal of High Energy Physics* **2023** no. 9, (2023) 74.
- [10] A. Raviv-Moshe and S. Zhong, “Phases of surface defects in scalar field theories,” *Journal of High Energy Physics* **2023** no. 8, (2023) 143.
- [11] G. Cuomo, Z. Komargodski, and A. Raviv-Moshe, “Renormalization group flows on line defects,” *Phys. Rev. Lett.* **128** (Jan, 2022) 021603.
- [12] G. Cuomo, Z. Komargodski, and M. Mezei, “Localized magnetic field in the $O(N)$ model,” *Journal of High Energy Physics* **2022** no. 2, (2022) 134.

- [13] O. Aharony, G. Cuomo, Z. Komargodski, M. Mezei, and A. Raviv-Moshe, “Phases of wilson lines in conformal field theories,” *Phys. Rev. Lett.* **130** (Apr, 2023) 151601.
- [14] O. Aharony, G. Cuomo, Z. Komargodski, M. Mezei, and A. Raviv-Moshe, “Phases of wilson lines: conformality and screening,” *Journal of High Energy Physics* **2023** no. 12, (2023) 183.
- [15] G. Cuomo and S. Zhang, “Spontaneous symmetry breaking on surface defects,” *Journal of High Energy Physics* **2024** no. 3, (2024) 22.
- [16] C. P. Herzog and N. Kobayashi, “The $O(N)$ model with ϕ^6 potential in $\mathbb{R}^2 \times \mathbb{R}^+$,” *JHEP* **09** (2020) 126, [arXiv:2005.07863 \[hep-th\]](#).
- [17] E. Lauria, P. Liendo, B. C. Van Rees, and X. Zhao, “Line and surface defects for the free scalar field,” *JHEP* **01** (2021) 060, [arXiv:2005.02413 \[hep-th\]](#).
- [18] C. P. Herzog and A. Shrestha, “Conformal surface defects in maxwell theory are trivial,” *Journal of High Energy Physics* **2022** no. 8, (2022) 282.
- [19] A. Gimenez-Grau, “Probing magnetic line defects with two-point functions,” [arXiv:2212.02520 \[hep-th\]](#).
- [20] L. Bianchi, D. Bonomi, and E. de Sabbata, “Analytic bootstrap for the localized magnetic field,” *JHEP* **04** (2023) 069, [arXiv:2212.02524 \[hep-th\]](#).
- [21] L. Bianchi, D. Bonomi, E. de Sabbata, and A. Gimenez-Grau, “Analytic bootstrap for magnetic impurities,” *Journal of High Energy Physics* **2024** no. 5, (2024) 80.
- [22] P. Dey and K. Ghosh, “Bootstrapping conformal defect operators on a line,” [arXiv:2404.06576 \[hep-th\]](#).
- [23] D. Rodriguez-Gomez, “A scaling limit for line and surface defects,” *Journal of High Energy Physics* **2022** no. 6, (2022) 71.
- [24] D. Rodriguez-Gomez and J. G. Russo, “Defects in scalar field theories, RG flows and dimensional disentangling,” *Journal of High Energy Physics* **2022** no. 11, (2022) 167.
- [25] I. Carreño Bolla, D. Rodriguez-Gomez, and J. G. Russo, “RG flows and stability in defect field theories,” *Journal of High Energy Physics* **2023** no. 5, (2023) 105.
- [26] T. Nishioka, Y. Okuyama, and S. Shimamori, “The epsilon expansion of the $O(N)$ model with line defect from conformal field theory,” *Journal of High Energy Physics* **2023** no. 3, (2023) 203.
- [27] S. Harribey, I. R. Klebanov, and Z. Sun, “Boundaries and interfaces with localized cubic interactions in the $O(N)$ model,” *Journal of High Energy Physics* **2023** no. 10, (2023) 17.
- [28] S. Harribey, W. H. Pannell, and A. Stergiou, “Multiscalar Critical Models with Localised Cubic Interactions,” [arXiv:2407.20326 \[hep-th\]](#).

- [29] J. Gomis, B. Le Floch, Y. Pan, and W. Peelaers, “Intersecting surface defects and two-dimensional CFT,” *Phys. Rev. D* **96** (Aug, 2017) 045003.
- [30] N. Drukker, M. Probst, and M. Trépanier, “Surface operators in the 6d $N = (2, 0)$ theory,” *Journal of Physics A: Mathematical and Theoretical* **53** no. 36, (Aug, 2020) 365401.
- [31] N. Drukker, Z. Kong, and G. Sakkas, “Broken global symmetries and defect conformal manifolds,” *Phys. Rev. Lett.* **129** (Nov, 2022) 201603.
- [32] M. Billo’, F. Galvagno, M. Frau, and A. Lerda, “Integrated correlators with a Wilson line in $\mathcal{N} = 4$ SYM,” *JHEP* **12** (2023) 047, [arXiv:2308.16575 \[hep-th\]](#).
- [33] M. Billò, M. Frau, F. Galvagno, and A. Lerda, “A note on integrated correlators with a Wilson line in $\mathcal{N} = 4$ SYM,” [arXiv:2405.10862 \[hep-th\]](#).
- [34] R. Dempsey, B. Offertaler, S. S. Pufu, and Y. Wang, “Global Symmetry and Integral Constraint on Superconformal Lines in Four Dimensions,” [arXiv:2405.10914 \[hep-th\]](#).
- [35] D. Karateev and B. Sahoo, “Correlation Functions and Trace Anomalies in Weakly Relevant Flows,” [arXiv:2408.16825 \[hep-th\]](#).
- [36] W. H. Pannell and A. Stergiou, “Line defect RG flows in the epsilon expansion,” *Journal of High Energy Physics* **2023** no. 6, (2023) 186.
- [37] I. Nagar, A. Sever, and D.-l. Zhong, “Planar RG flows on line defects,” *Journal of High Energy Physics* **2024** no. 6, (2024) 110.
- [38] W. H. Pannell, “A note on defect stability in $d = 4 - \varepsilon$,” [arXiv:2408.15315 \[hep-th\]](#).
- [39] V. Bashmakov and J. Sisti, “Exploring Defects with Degrees of Freedom in Free Scalar CFTs,” [arXiv:2410.01716 \[hep-th\]](#).
- [40] Z. Zhou and Y. Zou, “Studying the 3d Ising surface CFTs on the fuzzy sphere,” [arXiv:2407.15914 \[hep-th\]](#).
- [41] L. Hu, Y.-C. He, and W. Zhu, “Solving conformal defects in 3D conformal field theory using fuzzy sphere regularization,” *Nature Communications* **15** no. 1, (2024) 3659.
- [42] O. Diatlyk, Z. Sun, and Y. Wang, “Surprises in the Ordinary: $O(N)$ Invariant Surface Defect in the ϵ -expansion,” [arXiv:2411.16522 \[hep-th\]](#).
- [43] L. Bianchi, L. S. Cardinale, and E. de Sabbata, “Defects in the long-range $O(N)$ model,” [arXiv:2412.08697 \[hep-th\]](#).
- [44] J. L. Cardy and I. Peschel, “Finite-size dependence of the free energy in two-dimensional critical systems,” *Nuclear Physics B* **300** (1988) 377–392.
- [45] M. Henkel, A. Patkós, and M. Schlottmann, “The ising quantum chain with defects (i). the exact solution,” *Nuclear Physics B* **314** no. 3, (1989) 609–624.

- [46] D. Deutsch and P. Candelas, “Boundary effects in quantum field theory,” *Phys. Rev. D* **20** (Dec, 1979) 3063–3080.
- [47] J. L. Cardy, “Critical behaviour at an edge,” *Journal of Physics A: Mathematical and General* **16** no. 15, (Oct, 1983) 3617.
- [48] M. N. Barber, I. Peschel, and P. A. Pearce, “Magnetization at corners in two-dimensional ising models,” *Journal of Statistical Physics* **37** no. 5, (1984) 497–527.
- [49] A. J. Guttmann and G. M. Torrie, “Critical behaviour at an edge for the SAW and Ising model,” *Journal of Physics A: Mathematical and General* **17** no. 18, (Dec, 1984) 3539.
- [50] J. L. Cardy and S. Redner, “Conformal invariance and self-avoiding walks in restricted geometries,” *Journal of Physics A: Mathematical and General* **17** no. 17, (Dec, 1984) L933.
- [51] R. Z. Bariev, “Critical properties of a system near an angle boundary,” *Theoretical and Mathematical Physics* **69** no. 1, (1986) 1061–1062.
- [52] T. A. Larsson, “Ising model at an edge: a position space renormalisation group approach,” *Journal of Physics A: Mathematical and General* **19** no. 9, (Jun, 1986) 1691.
- [53] V. K. Saxena, “Percolation in an edge,” *Journal of Physics A: Mathematical and General* **20** no. 18, (Dec, 1987) 6623.
- [54] Z.-G. Wang, A. M. Nemirovsky, K. F. Freed, and K. R. Myers, “Effects of surface, wedge, corner, and mixed boundary conditions on the local critical behaviour,” *Journal of Physics A: Mathematical and General* **23** no. 12, (Jun, 1990) 2575.
- [55] F. Iglói, I. Peschel, and L. Turban, “Inhomogeneous systems with unusual critical behaviour,” *Advances in Physics* **42** no. 6, (1993) 683–740.
- [56] M. Pleimling and W. Selke, “Critical phenomena at edges and corners,” *The European Physical Journal B* **5** (01, 1998) .
- [57] M. Pleimling and W. Selke, “Edge critical behavior at the surface transition of ising magnets,” *Phys. Rev. B* **59** (Jan, 1999) 65–68.
- [58] M. Pleimling, “Phase transitions at surfaces, edges, and corners,” *Computer Physics Communications* **147** no. 1, (2002) 101–106. Proceedings of the Europhysics Conference on Computational Physics Computational Modeling and Simulation of Complex Systems.
- [59] N. Crampé and A. Trombettoni, “Quantum spins on star graphs and the kondo model,” *Nuclear Physics B* **871** no. 3, (2013) 526–538.

- [60] A. Antunes, “Conformal bootstrap near the edge,” *JHEP* **10** (2021) 057, [arXiv:2103.03132 \[hep-th\]](#).
- [61] A. Bissi, P. Dey, J. Sisti, and A. Söderberg, “Interacting conformal scalar in a wedge,” *JHEP* **10** (2022) 060, [arXiv:2206.06326 \[hep-th\]](#).
- [62] N. Drukker and M. Trépanier, “Ironing out the crease,” *Journal of High Energy Physics* **2022** no. 8, (2022) 193.
- [63] Griguolo, Luca and Guerrini, Luigi and Testa, Alessandro, “Into the wedge of $\mathcal{N} = 2$ superconformal gauge theories,” [arXiv:2411.04043 \[hep-th\]](#).
- [64] O. Diatlyk, H. Khanchandani, F. K. Popov, and Y. Wang, “Defect fusion and Casimir energy in higher dimensions,” *JHEP* **09** (2024) 006, [arXiv:2404.05815 \[hep-th\]](#).
- [65] O. Diatlyk, H. Khanchandani, F. K. Popov, and Y. Wang, “Effective Field Theory of Conformal Boundaries,” [arXiv:2406.01550 \[hep-th\]](#).
- [66] P. Kravchuk, A. Radcliffe, and R. Sinha, “Effective theory for fusion of conformal defects,” [arXiv:2406.04561 \[hep-th\]](#).
- [67] G. Cuomo, Y.-C. He, and Z. Komargodski, “Impurities with a cusp: general theory and 3d Ising,” [arXiv:2406.10186 \[hep-th\]](#).
- [68] H. Geng, S. Lüst, R. K. Mishra, and D. Wakeham, “Holographic BCFTs and communicating black holes,” *Journal of High Energy Physics* **2021** no. 8, (2021) 3.
- [69] R.-X. Miao, “Casimir effect and holographic dual of wedges,” *JHEP* **06** (2024) 084, [arXiv:2404.11783 \[hep-th\]](#).
- [70] X. Sun and S.-K. Jian, “Holographic dual of defect CFT with corner contributions,” [arXiv:2407.19003 \[hep-th\]](#).
- [71] T. Lai, Y.-W. Sun, and J. Tian, “Holographic correlation functions from wedge,” [arXiv:2411.12420 \[hep-th\]](#).
- [72] C. Bachas, J. de Boer, R. Dijkgraaf, and H. Ooguri, “Permeable conformal walls and holography,” *Journal of High Energy Physics* **2002** no. 06, (Jul, 2002) 027.
- [73] S. Fredenhagen and T. Quella, “Generalised permutation branes,” *Journal of High Energy Physics* **2005** no. 11, (Nov, 2005) 004.
- [74] A. B. Clark, D. Z. Freedman, A. Karch, and M. Schnabl, “Dual of the janus solution: An interface conformal field theory,” *Phys. Rev. D* **71** (Mar, 2005) 066003.
- [75] I. Brunner and D. Roggenkamp, “Defects and bulk perturbations of boundary landau-ginzburg orbifolds,” *Journal of High Energy Physics* **2008** no. 04, (Apr, 2008) 001.
- [76] D. Gaiotto, “Domain walls for two-dimensional renormalization group flows,” *Journal of High Energy Physics* **2012** no. 12, (2012) 103.

- [77] A. Konechny, “Renormalization group defects for boundary flows,” *Journal of Physics A: Mathematical and Theoretical* **46** no. 14, (Mar, 2013) 145401.
- [78] A. Konechny, “Fusion of conformal interfaces and bulk induced boundary RG flows,” *Journal of High Energy Physics* **2015** no. 12, (2015) 1–33.
- [79] G. Poghosyan and H. Poghosyan, “RG domain wall for the N=1 minimal superconformal models,” *Journal of High Energy Physics* **2015** no. 5, (2015) 43.
- [80] I. Brunner and C. Schmidt-Colinet, “Reflection and transmission of conformal perturbation defects,” *Journal of Physics A: Mathematical and Theoretical* **49** no. 19, (Apr, 2016) 195401.
- [81] A. Konechny, “RG boundaries and interfaces in Ising field theory,” *Journal of Physics A: Mathematical and Theoretical* **50** no. 14, (Mar, 2017) 145403.
- [82] A. Konechny, “Properties of RG interfaces for 2D boundary flows,” *Journal of High Energy Physics* **2021** no. 5, (2021) 178.
- [83] P. Brax and S. Fichet, “Casimir Forces in CFT with Defects and Boundaries,” *Physics* **6** (2024) 544–567, [arXiv:2312.02281 \[hep-th\]](#).
- [84] C. V. Coghurn, A. L. Fitzpatrick, and H. Geng, “CFT and lattice correlators near an RG domain wall between minimal models,” *SciPost Phys. Core* **7** (2024) 021.
- [85] S. Giombi, E. Helfenberger, and H. Khanchandani, “RG Interfaces from Double-Trace Deformations,” [arXiv:2407.07856 \[hep-th\]](#).
- [86] A. Polyakov, “Gauge fields as rings of glue,” *Nuclear Physics B* **164** (1980) 171–188.
- [87] A. G. Grozin, J. M. Henn, G. P. Korchemsky, and P. Marquard, “The three-loop cusp anomalous dimension in QCD and its supersymmetric extensions,” *Journal of High Energy Physics* **2016** no. 1, (2016) 140.
- [88] A. B. Zamolodchikov, “Renormalization Group and Perturbation Theory Near Fixed Points in Two-Dimensional Field Theory,” *Sov. J. Nucl. Phys.* **46** (1987) 1090.
- [89] S. Fredenhagen, M. R. Gaberdiel, and C. A. Keller, “Bulk-induced boundary perturbations,” *Journal of Physics A: Mathematical and Theoretical* **40** no. 1, (Dec, 2006) F17.
- [90] M. R. Gaberdiel, A. Konechny, and C. Schmidt-Colinet, “Conformal perturbation theory beyond the leading order,” *Journal of Physics A: Mathematical and Theoretical* **42** no. 10, (Feb, 2009) 105402.
- [91] S. Fredenhagen, M. R. Gaberdiel, and C. Schmidt-Colinet, “Bulk flows in virasoro minimal models with boundaries,” *Journal of Physics A: Mathematical and Theoretical* **42** no. 49, (Nov, 2009) 495403.

- [92] S. Shimamori, “Conformal field theory with composite defect,” *Journal of High Energy Physics* **2024** no. 8, (2024) 131.
- [93] D. Ge, T. Nishioka, and S. Shimamori, “Localized RG flows on composite defects and \mathcal{C} -theorem,” [arXiv:2408.04428 \[hep-th\]](#).
- [94] R. D. Pisarski, “Fixed-Point Structure of $(\phi^6)_3$ at Large N ,” *Phys. Rev. Lett.* **48** (Mar, 1982) 574–576.
- [95] E. Eisenriegler and H. W. Diehl, “Surface critical behavior of tricritical systems,” *Phys. Rev. B* **37** (Apr, 1988) 5257–5273.
- [96] M. Srednicki, *Quantum field theory*. Cambridge University Press, 1, 2007.
- [97] P. F. Byrd and M. D. Friedman, *Handbook of elliptic integrals for engineers and scientists*. 1971.